

ECOLOGY

Trophic signatures of seabirds suggest shifts in oceanic ecosystems

Tyler O. Gagne,¹ K. David Hyrenbach,² Molly E. Hagemann,³ Kyle S. Van Houtan^{1,4*}

Pelagic ecosystems are dynamic ocean regions whose immense natural capital is affected by climate change, pollution, and commercial fisheries. Trophic level–based indicators derived from fishery catch data may reveal the food web status of these systems, but the utility of these metrics has been debated because of targeting bias in fisheries catch. We analyze a unique, fishery-independent data set of North Pacific seabird tissues to inform ecosystem trends over 13 decades (1890s to 2010s). Trophic position declined broadly in five of eight species sampled, indicating a long-term shift from higher–trophic level to lower–trophic level prey. No species increased their trophic position. Given species prey preferences, Bayesian diet reconstructions suggest a shift from fishes to squids, a result consistent with both catch reports and ecosystem models. Machine learning models further reveal that trophic position trends have a complex set of drivers including climate, commercial fisheries, and ecomorphology. Our results show that multiple species of fish-consuming seabirds may track the complex changes occurring in marine ecosystems.

INTRODUCTION

Robust indicators of ecosystem health are critical to understand threats, guide management of resilience, and promote sustainability in marine ecosystems (1, 2). Because food web dynamics capture both species and their ecosystem interactions (3, 4), they are a common means to assess ecosystem status. One such intuitive indicator used for commercial fisheries is the mean trophic level (MTL). At the global scale, MTL shows or obscures a variety of trends and signals including the overharvesting and collapse of large predators [“fishing down food webs”; (5)] and the proliferation of fisheries targeting low-TL species [“fishing through food webs”; (6)]. This metric has been challenged as a true indicator of ecosystem status, however, because MTL is generated from commercial catch data that incorporate a wide array of biases (7). Developing TL metrics from fishery-independent data, as a result, could advance the sustainable management of marine ecosystems (8).

An increasingly popular technique, compound-specific stable isotope analysis of $\delta^{15}\text{N}$ in amino acids (CSIA-AA), holds promise for developing ecosystem indicators (9). Embedded within the tissues of most organisms is a memory of their ecosystem experience (10). Age, biogeography, diet, and other relationships can be described through a variety of tissue tracers (11–14). CSIA-AA is unique in that it compares the relative enrichment of ^{15}N to ^{14}N ($\delta^{15}\text{N}$) in trophic and source amino acids, building upon earlier bulk stable isotope methods, by yielding a robust and unbiased estimate of an organism’s trophic position (TP) (9, 15). Applications of this technique to date, however, have largely addressed single species questions (16–20) or food web models (15, 21). CSIA-AA has not been applied to a fishery-independent data stream to assess marine ecosystem status over time or to test the various drivers of the observed trends.

Here, we examine whether broad shifts in food web structure are reflected in a 125-year time series of seabird tissues from the central North Pacific. As a taxon, seabirds may serve as good indicators of marine ecosystem trophic state (22). To begin, seabirds represent a diverse

array of high-TL fish consumers capable of integrating much of an ecosystem’s food web dynamics. Foundational research using bulk stable isotopes suggested that the seabird TP may track prey availability (19, 20). However, the results of those studies can be questioned because of the sensitivity of bulk isotopes to shifts at the ecosystem base, due to changing ocean productivity and nutrient recycling (23, 24). Further development with multispecies approaches shows promise, as seabirds exhibit a wide array of foraging strategies, prey selection, and geographic affinities that provide a diverse perspective to document and analyze environmental change (25). On a practical level, seabird specimens are readily accessed at large breeding colonies, from fishery bycatch and strandings, and, importantly, are well represented in natural history collections.

We use CSIA-AA to determine the TP of eight seabird species through time (1891 to 2016). First, we describe the historical trends, interpret the differences among species, and use hierarchical models to estimate prey shifts given established dietary preferences. Next, we use random forest algorithms (RFs) to quantify the relative importance of climate, commercial fisheries, and ecomorphology to long-term TP changes. Our results provide new insights into trophic web dynamics in pelagic ocean basins over time and highlight the potential of using CSIA-AA-derived TPs in seabirds as a meaningful indicator of ecosystem status. These multispecies, fishery-independent indicators may inform ecosystem-based management (26).

RESULTS

Seabird TP declines broadly

Seabird TPs declined broadly over 125 years in the central North Pacific (Fig. 1). Solid lines are model medians with 95% credible intervals for eight species (blue) and an all-species ensemble (red). As evidenced by the baseline values from 1890 (dashed line), five of eight species show clear declines (Fig. 1, B, C, E, G, and H), two species oscillate (Fig. 1, D and F), and one remains constant (Fig. 1A). TP does not increase in any species. For brown noddy (BRNO) and white-tailed tropicbird (WTTR), TP oscillates near 1983, proximate significant El Niño–Southern Oscillation (ENSO) (27) and regime shift (28) events. We observed a similar oscillation during this period in the diet reconstruction model, which may suggest that prey dynamics in the preferred foraging areas of these species bear an ENSO signal.

Copyright © 2018
The Authors, some
rights reserved;
exclusive licensee
American Association
for the Advancement
of Science. No claim to
original U.S. Government
Works. Distributed
under a Creative
Commons Attribution
NonCommercial
License 4.0 (CC BY-NC).

¹Monterey Bay Aquarium, 886 Cannery Row, Monterey, CA 93940, USA. ²Hawaii Pacific University, 45-045 Kamehameha Highway, Kaneohe, HI 96744, USA. ³Vertebrate Zoology Collections, Bernice Pauahi Bishop Museum, 1525 Bernice Street, Honolulu, HI 96817, USA. ⁴Nicholas School of the Environment, Duke University, Box 90328, Durham, NC 27708, USA.

*Corresponding author. Email: kvanhoutan@mbayaq.org

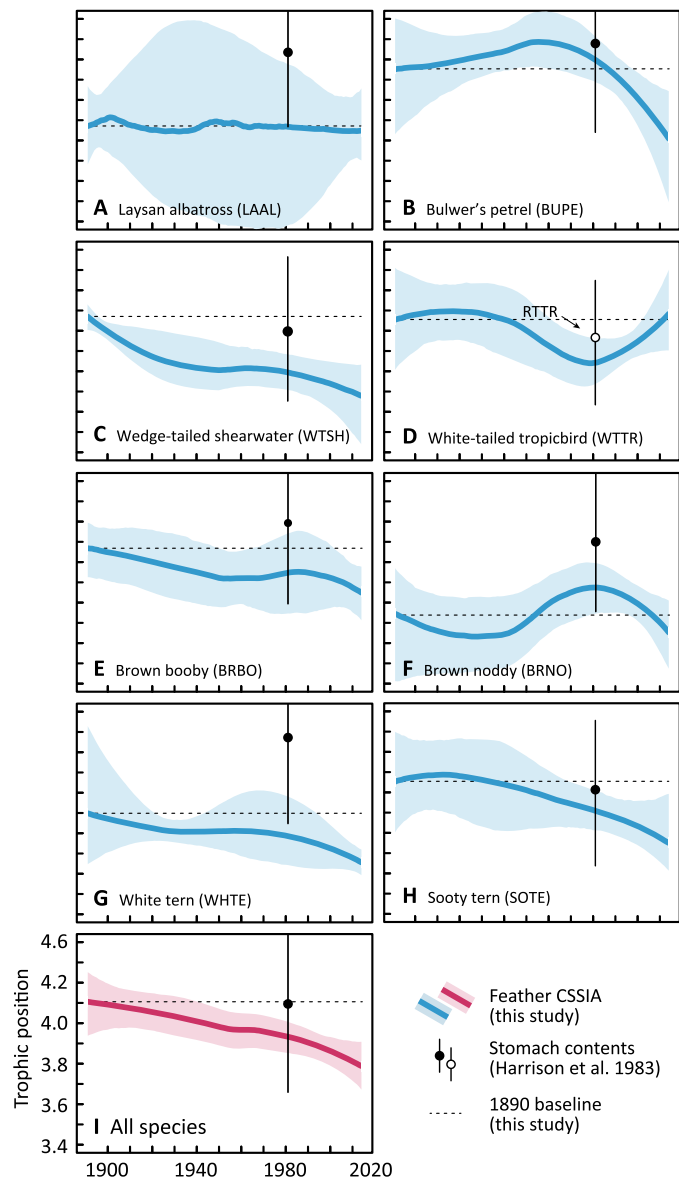


Fig. 1. Seabird TP declined broadly from 1890 to the present. (A to H) Individual seabird species TP series (blue lines) generated from CSIA-AA in feathers. (I) All species TP unweighted mean ensemble (red line). Lines are median model output; shaded area is the 95% credible interval. Circles plot point estimates of the TL computed from the observed stomach contents (29) and forage species MTL (15, 50); thick black lines are SE. Dotted horizontal line is the baseline TP value calculated in 1890. TP declines overall from 4.1 to 3.8 during this period, with the decline from 1950 to the present being twice the rate as before. Where most species showed declines (B to E, G, and H; 63%), two fluctuated over time (D and F; 25%) and one remained remarkably constant (A; 13%). CSSIA, compound specific stable isotope analysis; RTTR, red-tailed tropicbird.

Additionally, we compare these CSIA-AA-derived values to point estimates (circles, plotted at 1980) of TL estimates based from diet (Fig. 2) (29). Although within the range of error, CSIA-AA-derived TP values are consistently below point TL estimates. This may arise as low-TL noncalcified or nonbony species are poorly detected in stomach content studies (30, 31) on which TL estimates are often based. CSIA-AA of tissues, however, is free from this bias. Such a mismatch may also occur because the tissue assimilation of dietary nitrogen occurs over a longer-

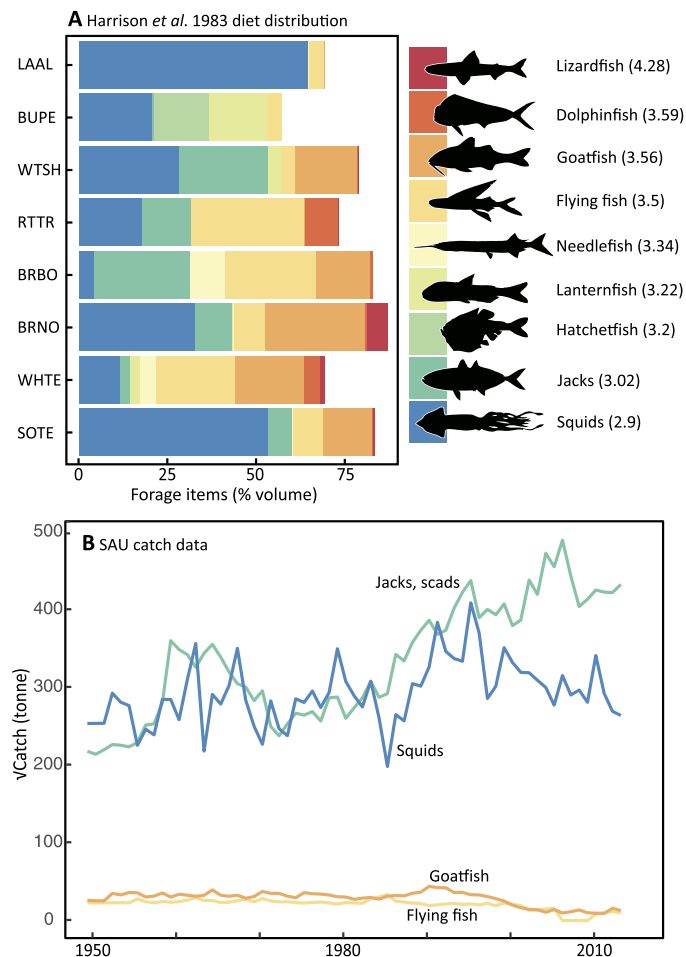


Fig. 2. Seabird prey species and their commercial landings. (A) Taxa represented in seabird diets observed from stomach contents (29) for all prey comprising >5% diet volume. This yields forage proportions, and we list MTL (parentheses) for each group. Squids, goatfish, flying fish, and jacks are the dominant prey (volume, 65%). (B) Commercial landings reconstructed (58) from spatially explicit catch records for the dominant prey taxa above, available from 1950 to the present. Y axes are square root-transformed to aid visualization.

term period (months), whereas stomach contents reflect the most recent (hours to days) organismal activity. However, if this were affecting our study, then we might see diet-derived values randomly positioned and not consistently above CSIA-AA-derived estimates.

From 1891 to 2016, the ensemble decline in TP was 0.32 (table S1), similar to decreases in the Hawaiian petrel (*Pterodroma sandwichensis*) observed at a millennial time scale (17). The ensemble decline from 1950 to 2016 (0.20) nearly doubled the rate during the first half of the time series 1891 to 1950 (0.13). Wedge-tailed shearwater (WTSH), a reported sentinel species (22), showed the steepest decline (0.38). Despite large credible intervals, Laysan albatross show a remarkably stable TP. Figure S2 provides full model randomizations and estimates.

Diet abundance of squid doubles

Historical prey reconstructions from hierarchical Bayesian mixing models indicate a marked increase in squids and a decline in four fish families (Fig. 3). Although individual species patterns vary, the ensemble (Fig. 3I) shows that squid almost doubles (22 to 42%), hatchetfish and lantern fish

decline (38 to 29%), flying fish and goatfish decrease by 50% (29 to 14%), and jacks remain stable (11 to 15%). Incidentally, nearshore catch and market data from Hawaii also indicate a marked decline in jacks during this period (32). Species with little TP changes, such as BRNO and Laysan albatross (LAAL), demonstrated a relatively consistent diet across the study period. Overall, the Gelman-Rubin diagnostic of convergence was <1.05 for 96.8% of the variables, indicating model confluence.

Ecomorphology of study species varied widely

The eight seabird species we studied display a variety of ecomorphology strategies (Fig. 4). Wing tracings reveal differences in size and form (Fig. 4A), from which we calculate flight aerodynamic metrics including wing area (Fig. 4B) as well as aspect ratio and wing loading (Fig. 4C).

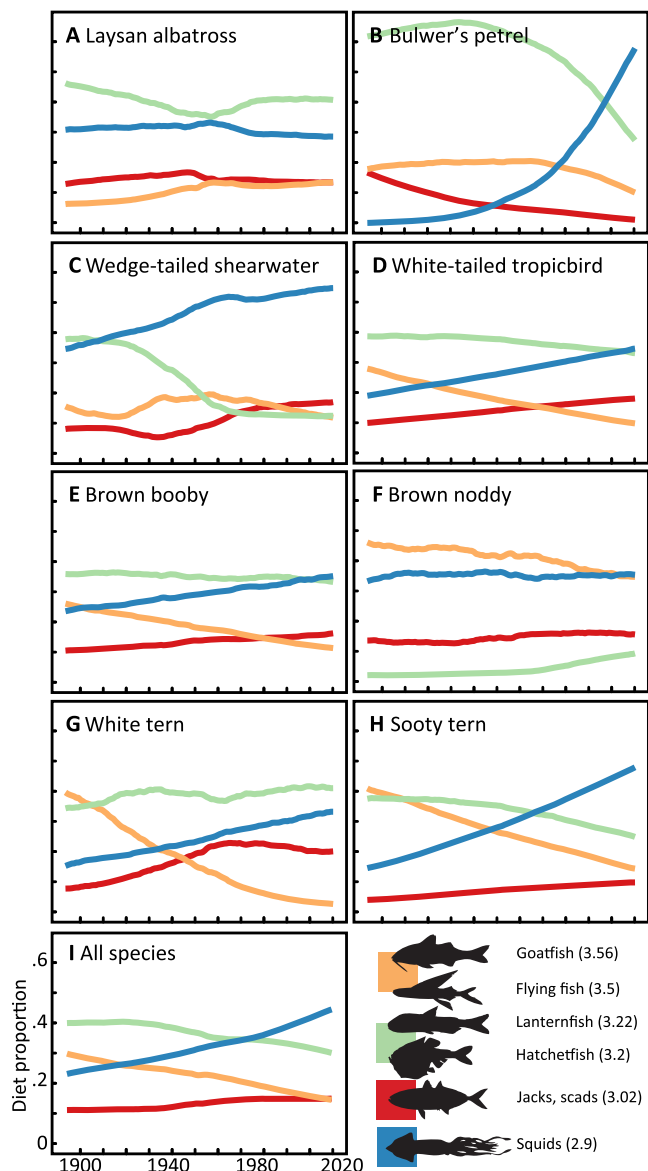


Fig. 3. Diet reconstructions show a shift from fish to squids. Bayesian mixing model outputs that reconstruct diet composition longitudinally using CSIA-derived TP (Fig. 1) and prey item TL (fig. S6) for individual species (A to H) and averaged across species (I). We combined four taxa into two diet groups due to TL similarities. The resulting groups encompass six taxa comprising the majority (>80%) of diet volume (29).

Function follows form. On the basis of model deviations, Laysan albatross (LAAL) have relatively large wings with low loadings (Fig. 4, B and C), yielding efficient flight (33) capable of exploiting large foraging areas (Fig. 4, D and E). Conversely, brown booby (BRBO) has high wing loading (Fig. 4C) and limited at-sea foraging capability (Fig. 4, D and E). Of the species we examined, Laysan albatross are uniquely capable of reaching the transition zone chlorophyll front, an important productivity hotspot (34).

Prey availability, climate, and ecomorphology drive trophic dynamics

The 10 most important model inputs influencing TP in descending order are as follows: forage distance, jacks catch, goatfish catch, squid catch, wing loading, Pacific Decadal Oscillation (PDO) lag-1, North Pacific Gyre Oscillation (NPGO) index, multivariate ENSO index (MEI) lag-1, sea surface temperature (SST), and PDO (Fig. 4A). (We exclude species and year from this list to facilitate interpretation; fig. S14.)

The full RF model explained 63% of the TP variance and had strong agreement between predicted and observed values of the test data. The root mean square error (RMSE) of the full model was 0.169 TP, which is an average prediction error 4.4% off the average observed TP. For comparison, the climate-only model test set RMSE was 0.211, 0.262 for species/ecomorphology-only model, 0.218 for the catch data-only model, and 0.218 for the year-only model (table S4). Partial dependence plots (Fig. 4B) show TP increases with increases in foraging distance, goatfish catch, squid catch, PDO lag, NPGO, MEI lag, and SST. TP declines with jacks catch, wing loading, PDO, SST, and MEI increases. Partial dependence surfaces (Fig. 4C) show interactive variable relationships. For example, species with low wing loading and high forage distance are most likely to have the highest relative TP. Additionally, specific climate scenarios appear tied to high TP. Several of these plots show the importance of squid catch.

It is important to interpret the partial dependence outputs in Fig. 5 (B and C) and figs. S10 to S12 with caution. Partial dependence plots can illustrate conditional relationships in two- or three-dimensional space using a response surface. However, because RF models can distinguish multivariate interactions, it is essential to note that such plots, although powerful, may not entirely reveal the interactions of the predictor variables. The two-dimensional partial dependence plot of wing loading (Fig. 5B) exemplifies this point. Although wing loading weights are highly important (Fig. 5A and fig. S13), its relative conditional effect size appears small (Fig. 5B), likely due to its interactions with other important variables across the species ensemble. Detailed insights into these interactions may be gathered from the individual conditional expectation plots in the Supplementary Materials (see fig. S11).

DISCUSSION

Where previous studies (5–7) rely largely on a combination of fishery-dependent data and fish diets or focus on single species and use older methodologies that can be questioned (19, 20), we used CSIA-AA to analyze stable isotopes embedded within the tissues of eight different species of seabirds. This enabled us to generate a fishery-independent index of TP for eight marine predators for over 125 years, which both avoids the known biases inherent in catch data (6, 7) and extends the timeline of analysis beyond the catch data period (since 1950). We demonstrate that TP declined broadly in the North Pacific from 1890 to the present (Fig. 1), likely due to a decrease in high-TL fish and an increase in low-TL squid (Fig. 3). RF models (Fig. 5) indicate that these changes

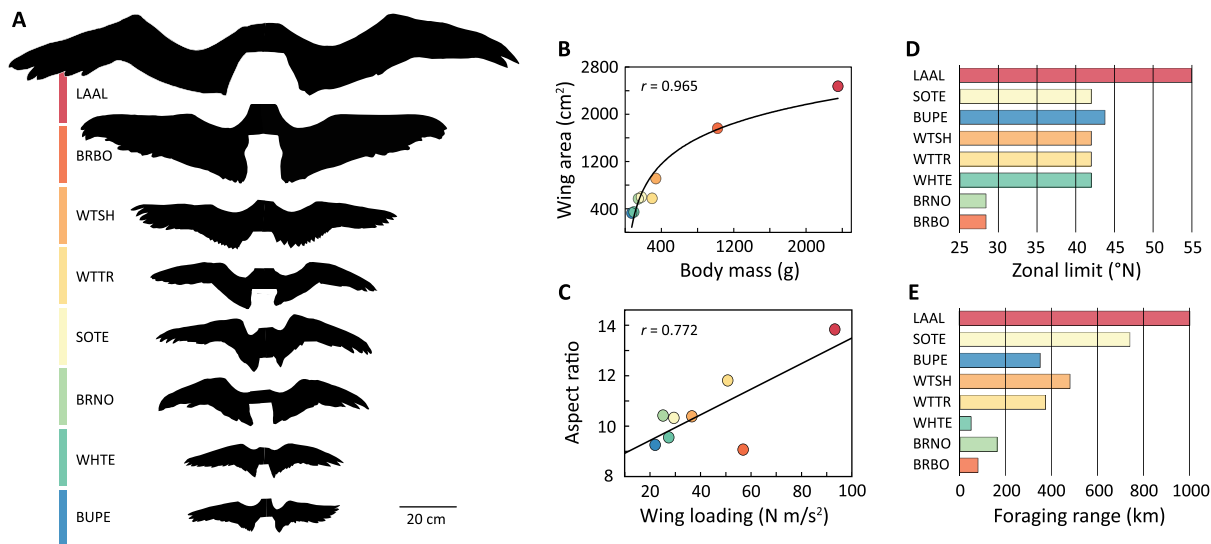


Fig. 4. Ecomorphology reveals unique structure and foraging strategies. Wing tracing silhouettes (A) and various aerodynamic metrics for seabirds in this study (B and C). Observed foraging distances in the North Pacific, plotted as (D) northern latitudinal limits and (E) absolute distances from breeding areas. LAAL have a relatively high wing area per body mass (B) and relatively high aspect ratio per wing loading (C), enabling extended forage bouts at sea (D and E). Conversely, BRBO has a relatively high wing loading per wing aspect (C), limiting its pelagic flights (D and E). Species color codes are retained through all panels.

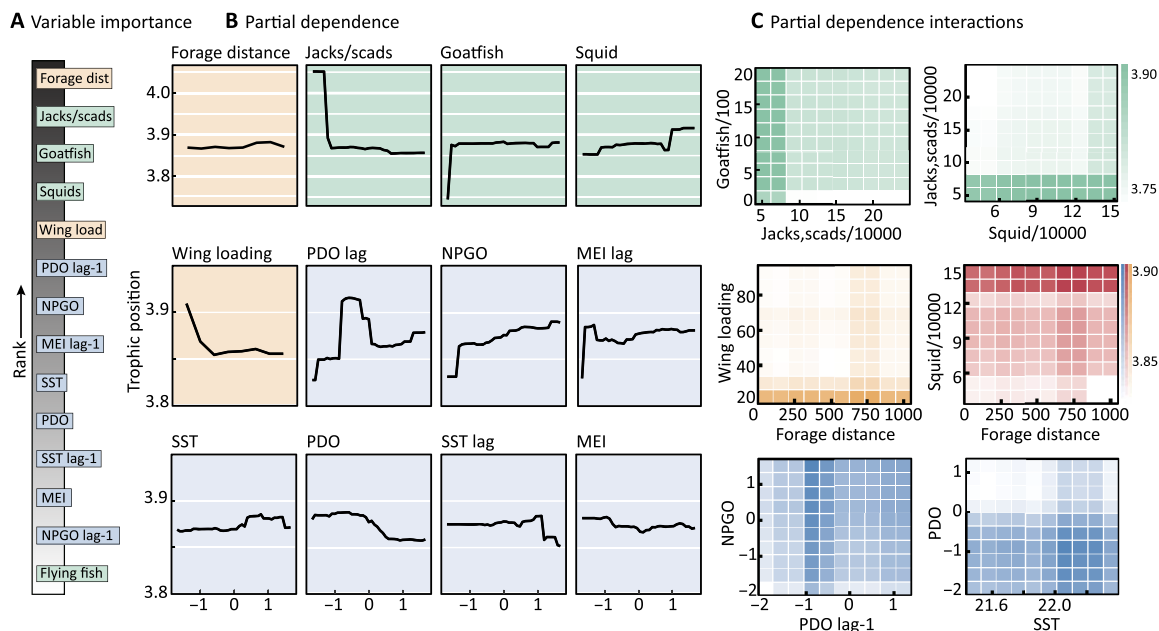


Fig. 5. Random forest variable importance and partial dependence plots. (A) Ranked predictors by measure of the variable importance. Variable importance is the measure by which the model mean square error (MSE) is reduced if the variable is randomly permuted. (B) Partial dependence plots for the top 12 predictors in order of variable importance. The plots show the TP response relative to a predictor when all other predictors are mediated for. Yellow subpanels are ecomorphological traits, green subpanels are reconstructed fishery predictors, and blue subpanels are climate inputs. (C) Partial dependence surface plots; all color designations hold except for the red subpanel, which is a cross-sectional interaction. Notable (B) partial dependence plots are the high TPs observed for species with low wing loading, years of low jacks and scads catch, periods of high squid capture, and periods of high NPGO index values. On the surface plots (C), relatively high TPs are observed for species with low wing loading and high forage distances, periods of high SST, and lower PDO index values.

are due not only to commercial fishing but also to a complex interaction of ecomorphology (Fig. 4), prey availability (Fig. 2), and climate (fig. S4) factors.

Are seabirds fishing down marine food webs? From 1950 to 1995, the seabird TP declines we observed are similar to the reported changes

in global catch MTL [0.2; (5)] but more pronounced than the estimated MTL for the North Pacific alone (0.05). Subsequent catch analyses (7) suggest that global MTL may have increased from 1980 to 2015, which we found in only one of eight species in that period. The dominant species pattern we documented was declining or stable TP (Fig. 1). The

species ensemble model shows a gradual rate of decline in TP over time that doubles after 1950 (table S1) or during the rise of industrial fishing. Although CSIA-AA has been used variously (9, 15, 16, 35) to estimate TP, our results do not appear sensitive to different formulations of TP from CSIA-AA data (see fig. S3). Because many of these seabird populations we analyze are rebounding from historical bottlenecks (36), their aggregate fishing power may not approach that of commercial fisheries over this period. However, more research in this area is needed. Studies at global (37) and basin (38) scales suggest that seabirds consume prey biomass on par with commercial fisheries. However, such models often extrapolate fine-scale temporal observations during the breeding season, when seabirds provision their chicks, and thus are subject to propagation errors and large model uncertainties.

Bayesian diet reconstructions displayed a visible shift from fishes to squids (Fig. 3). This result is sensitive to prey TL (fig. S8), and we further assume that prey TLs are themselves consistent over the study period. Future modeling efforts might examine how pervasive trophic downgrading or shifts in prey size distributions (39) might influence trends in predator TPs. Despite these assumptions, TP determined by CSIA-AA is considered insensitive to shifts at the base of the food web (9) and to basin scale N cycling dynamics (17). Our diet reconstruction aligns with the global expansion in cephalopods (40, 41) and with the declining catch of high-TL flying fish and goatfish (Fig. 2B).

In line with a hierarchical theory of ecological indicators (8), model outputs show that ecomorphology and prey availability have direct and dominant influences on TP, and that climate also factors (Fig. 5A). Both the partial dependence (Fig. 4B) and variable interaction plots (Fig. 5C) reveal a complex set of nonlinear relationships. The direction of these relationships and the underlying mechanisms rely largely on how catch data might reflect actual abundance. For goatfish, TP increases with catch, and therefore, we might expect goatfish landings (TL = 3.56) to reflect abundance. Given that Hawaii-based goatfish catch has dropped (32), TP for goatfish consumers might correspondingly also decline due to dietary replacement. Squid abundance is notoriously unpredictable (41). The positive model relationship between squid catch and TP that we find may reflect provisioning for fish that are seabird prey. Generally, the lagged climate series are higher ranked than the raw data (Fig. 5B), which may indicate that climatic forcing of prey abundance is not immediate. From ecomorphology, the highest TP occurs in species with low wing loading and high forage ranges, who might search large regions efficiently for high-TL targets.

A few of the seabird species that we study here [sooty tern (SOTE), BRNO, and WTSH] forage in association with predatory fish schools (42). The failure of such fisheries in certain locations has seen a commensurate response in some seabird diets (43, 44). Our predictive models for TP across time incorporate a variety of drivers (climate, ecomorphology, and fisheries) that can influence all eight seabird species. The catch data comprising our model inputs (Fig. 2) essentially assess competitive exclusion by commercial fisheries, and not the commensal relationship whereby predatory fish like tunas concentrate seabird prey close to the ocean surface. Such dynamics would be better assessed by quantifying the concurrent availability of spatially explicit catch and the movements of tuna-associated seabirds across time. Although insufficient data exist at this time, a combination of active acoustic and microtag tracking (44–46) may help better understand how the commercial catch of tunas affects tuna-associated seabirds.

Being central-place foragers (22, 47), seabirds may maximize foraging efficiency (48) yet respond opportunistically to prey availability at sea. Therefore, we expect that the seabird TPs we observe integrate the

various ecosystem factors that determine the distribution and abundance of prey, ultimately reflecting and approximating ecosystem status. Although the data and methods presented here may resolve some issues posed by catch MTL, essentially replacing human predators with seabirds and diet studies with CSIA-AA, understanding seabird TP patterns themselves ultimately relies on true fish abundance trends. These data, although important, are both logistically demanding and elusive (1, 7). The replication of our analysis in other regions, through available historical specimens, may also hold insights into the status of marine ecosystems and the future of seabird populations.

METHODS

Sample collection and isotope analyses

We obtained feathers for eight seabird species from the Hawaiian archipelago: Laysan albatross (*Phoebastria immutabilis*), Bulwer's petrel (*Bulweria bulwerii*), wedge-tailed shearwater (*Puffinus pacificus*), white-tailed tropicbird (*Phaethon lepturus*), brown booby (*Sula leucogaster*), brown noddy (*Anous stolidus*), white tern (*Gygis alba*), and sooty tern (*Sterna fuscata*). Specimens dated from 1891 to 2016 were sourced from museum archives and necropsies of wild birds [$n = 134$; U.S. Fish and Wildlife Service (USFWS) permits MB052060-0 and MB180283-1]. To minimize impacts to historical specimens, we accessed body contour feathers along the sides and flanks. For contemporary specimens, we sampled fully emerged flight feathers. Specimen availability determined sample abundance (minimum, 10 feathers per species; average, 17; maximum, 24). We homogenized specimens and sent samples to the UC Davis Stable Isotope Facility for CSIA-AA.

CSIA-AA and diet composition (29) calculated species TP and TL, respectively. TP represents

$$TP = \frac{(\delta^{15}N_{TTP} - \delta^{15}N_{Src} - \beta)}{TEF} + 1$$

where $\delta^{15}N_{TTP}$ is the average $\delta^{15}N$ value for the six trophic AAs and $\delta^{15}N_{Src}$ is the $\delta^{15}N$ value for the source AA. β (=2.42) and TEF (=5.63) are AA-specific constants, averaged from each trophic AA (9). We generated random TP values from CSIA-AA parameters and generated time series by fitting a locally weighted regression (49) to randomized TP estimates for each sample. We repeated the process 1000 times for each series to generate medians and credible intervals.

Prey item composition and longitudinal record

The only exhaustive survey (29) of these species diets provided prey composition during 1978 to 1980. Samples were regurgitates collected in the Northwestern Hawaiian Islands from 1978 to 1980. We substituted red-tailed tropicbirds (*Phaethon rubricauda*) for white-tailed tropicbirds, because the latter are unavailable, and both species are solitary foragers that target epipelagic prey. Species otherwise self-represent. We sourced spatially reconstructed catch data for major prey taxa from the Sea Around Us (SAU) database (2, 39). This provided data for the seabird foraging area (10° to 44°N, 140° to 235°W) for Carangidae (jacks), Exocoetidae (flying fish), Mullidae (goatfish), and Ommastrephidae (flying squids). These four taxa (fig. S9) constituted 65% of the mean diet volume for the seabirds we studied. SAU reconstructs catches through composites of Food and Agriculture Organization of the United Nations (FAO) data with best estimates of unreported catch, both landed and discarded. Catch distribution was approximated through

FAO area presence, latitudinal range, range-limited polygon generation, depth range, habitat preference, and equatorial submergence. In the absence of catch-per-unit-effort data, catch data may approximate fishing pressure and relative abundance (1).

A recent analysis (15) provided invertebrate TL. We calculated seabird TL as a function of stomach contents using

$$TL = \left(\sum_{j=1}^n P_j \times TL_j \right) + 1$$

where P_j is the proportion of the j th food item based on the literature dietary data and TL_j is the MTL of the j th prey item family (15, 50). We plotted TL estimates at 1980 over the fitted TP series (Fig. 1). Hierarchical Bayesian mixing models (Supplementary Methods) generated prey proportions over time, using prey TL to reconstruct the TP series.

Historical diet reconstruction

We used hierarchical Bayesian mixing models [R package MixSIAR; (51)] to visualize shifts in diet proportions of prey sources across time. In this model, the TP values in Fig. 1 are the mixture biotracer response as a function of prey item assimilation, where the TL of six prey items was the source biotracer input. Year was as a continuous random effect. Uncertainty in source data TL was built in using mean and SE of the TL from the literature and FishBase. We used a process error structure to account for variation in seabird TLs (52). This structure permits consumers to sample in different locations from each prey source distribution, and subsequent variation in consumer tracer values is accounted for in this sampling process. We fixed discrimination factors to 1 because TL magnification from prey to predator is 1.

We generated informative Dirichlet priors with the weight of an uninformative prior from the mean prey contribution estimates across the eight seabird species (29). The sum of the Dirichlet hyperparameters is equivalent in weight to the number of source groups (that is, four for four source groups; fig. S5). We ran the mixing model for three chains over 100,000 iterations, removing 50,000 for burn-in and thinning by a factor of 50. Gelman-Rubin diagnostics assessed convergence.

Climate record

We selected four basin-wide climate indices for model inputs (fig. S4). These were the MEI, PDO, NPGO, and North Pacific SST. The extended MEI was the calendar year means of the bimonthly index of SST and sea surface height anomalies in the tropical Pacific from 1890 to the present (27). The PDO series are the calendar year means of the bimonthly index values of the first empirical orthogonal function (EOF) of SST and sea surface height from 1890 to the present [National Oceanic and Atmospheric Administration (NOAA) National Centers for Environmental Information]. The NPGO series are the calendar year means of the monthly index values from 1950 to the present of the second EOF of SST and sea surface height (53). The Extended Reconstructed SST v4 (ERSST) is the global monthly SST data set from the International Comprehensive Ocean-Atmosphere Data Set (ICOADS) (54). We averaged a subset grid of the region encompassing the maximum study species foraging range (10° to 44°N, 140° to 235°W) and calculated calendar year means to build the series. To address ecosystem responses to climate changes, we generated lagged climate series, where climate data from a given time period (t) are used to model the trophic data from the following time period ($t + 1$). Because the trophic signature turnover in feathers is a subannual process, we used a 1-year lag.

Random forest model predictions

We used RF models to interpret the strength and nature of relationships between TP and prey availability, ecomorphology, and climate (55). RF offers a modeling strategy that is robust while still amiable to interpretation similarly to more familiar parametric models. However, RF is resilient to large numbers of correlated predictors and nonlinear relationships (56). In contrast to conventional parametric models, algorithmic models like RF do not require a priori assumption of the predictor-response relationship, but rather learn the form of those relationships (57) through data splitting. RF constructs multiple regression trees that can identify irregular patterns, along with linear, curvilinear, or step-wise relationships (57). Although individual regression trees may overfit data, RF overcomes this shortcoming by “averaging” an entire “forest” of regression trees that are trained on different subsets of predictors and response values. Each tree is generated through bootstrap samples, where one-third of the sample is left out for validation with out-of-bag prediction. Powerful trees can be extracted individually from a forest, although the resiliency of RF lies in interpreting the whole forest ensemble model output. To minimize overfitting concerns, we used a conservative hyperparameter parameterization, the number of trees in our model (ntree) was 2000, and the minimum terminal node size for individual trees was set at 5. The number of predictors available for splitting at each tree node (mtry) was set at the algorithm convention of the number of parameters divided by three rounded down ($K/3$).

We interpreted RF regressions with partial dependence plots. These plots show predicted values of a response variable along a gradient of an explanatory variable while, importantly, conditioning for all other explanatory variables. In addition, because variable importance (Fig. 5A and fig. S13) metrics are useful at interpreting predictive power of independent variables, we used the reduction in MSE of a model when a predictor is randomly permuted. RMSE and explained variance (R^2) evaluate overall model performance.

SUPPLEMENTARY MATERIALS

Supplementary material for this article is available at <http://advances.sciencemag.org/cgi/content/full/4/2/eaao3946/DC1>

Additional Methods

Additional Results

fig. S1. Mean absolute TP change.

fig. S2. TP data simulation raw output.

fig. S3. TP by measure of phenylalanine and glutamic acid only.

fig. S4. Incorporated climate indices.

fig. S5. Informative Dirichlet priors.

fig. S6. Hierarchical mixing model source distributions.

fig. S7. Mixing model output with confidence bands.

fig. S8. Faceted graphs of reconstructed SAU fishery catch time series.

fig. S9. Partial dependence plots of random forest model output with FAO data.

fig. S10. Partial dependence plots of random forest model output with SAU data.

fig. S11. Individual conditional expectation plots.

fig. S12. Partial dependence surface plots.

fig. S13. Full random forest variable importance output.

table S1. Mean absolute TP change.

table S2. Top 100 linear mixed-effects models.

table S3. Top 10 linear models by species.

table S4. Random forest model performance.

REFERENCES AND NOTES

1. D. Pauly, R. Hilborn, T. A. Branch, Fisheries: Does catch reflect abundance? *Nature* **494**, 303–306 (2013).
2. D. P. Tittensor, M. Walpole, S. L. L. Hill, D. G. Boyce, G. L. Britten, N. D. Burgess, S. H. M. Butchart, P. W. Leadley, E. C. Regan, R. Alkemade, R. Baumung, C. Bellard,

- L. Bouwman, N. J. Bowles-Newark, A. M. Chenery, W. W. L. Cheung, V. Christensen, H. D. Cooper, A. R. Crowther, M. J. R. Dixon, A. Galli, V. Gaveau, R. D. Gregory, N. L. Gutierrez, T. L. Hirsch, R. Höft, S. R. Januchowski-Hartley, M. Karmann, C. B. Krug, F. J. Leverington, J. Loh, R. K. Lojenga, K. Malsch, A. Marques, D. H. W. Morgan, P. J. Mumby, T. Newbold, K. Noonan-Mooney, S. N. Pagad, B. C. Parks, H. M. Pereira, T. Robertson, C. Rondinini, L. Santini, J. P. W. Scharlemann, S. Schindler, U. R. Sumaila, L. S. L. Teh, J. van Kolck, P. Visconti, Y. Ye, A mid-term analysis of progress toward international biodiversity targets. *Science* **346**, 241–244 (2014).
3. V. Christensen, D. Pauly, ECPATH II—A software for balancing steady-state ecosystem models and calculating network characteristics. *Ecol. Model.* **61**, 169–185 (1992).
4. S. L. Pimm, *Food Webs* (Chapman & Hall, 1982), p. 219.
5. D. Pauly, V. Christensen, J. Dalsgaard, R. Froese, F. Torres Jr., Fishing down marine food webs. *Science* **279**, 860–863 (1998).
6. T. E. Essington, A. H. Beaudreau, J. Wiedenmann, Fishing through marine food webs. *Proc. Natl. Acad. Sci. U.S.A.* **103**, 3171–3175 (2006).
7. T. A. Branch, R. Watson, E. A. Fulton, S. Jennings, C. R. McGilliard, G. T. Publico, D. Ricard, S. R. Tracey, The trophic fingerprint of marine fisheries. *Nature* **468**, 431–435 (2010).
8. R. F. Noss, Indicators for monitoring biodiversity: A hierarchical approach. *Conserv. Biol.* **4**, 355–364 (1990).
9. J. M. Nielsen, B. N. Popp, M. Winder, Meta-analysis of amino acid stable nitrogen isotope ratios for estimating trophic position in marine organisms. *Oecologia* **178**, 631–642 (2015).
10. K. S. Van Houtan, A. H. Andrews, T. T. Jones, S. K. K. Murakawa, M. E. Hagemann, Time in tortoiseshell: A bomb radiocarbon-validated chronology in sea turtle scutes. *Proc. R. Soc. B* **283**, 20152220 (2016).
11. J. T. Christensen, K. Richardson, Stable isotope evidence of long-term changes in the North Sea food web structure. *Mar. Ecol. Prog. Ser.* **368**, 1–8 (2008).
12. J. Dalsgaard, M. St. John, G. Kattner, D. Müller-Navarra, W. Hagen, Fatty acid trophic markers in the pelagic marine environment. *Adv. Mar. Biol.* **46**, 225–340 (2003).
13. S. G. DuBay, C. C. Fuldner, Bird specimens track 135 years of atmospheric black carbon and environmental policy. *Proc. Natl. Acad. Sci. U.S.A.* **114**, 11321–11326 (2017).
14. S. E. Swearer, J. E. Caselle, D. W. Lea, R. R. Warner, Larval retention and recruitment in an island population of a coral-reef fish. *Nature* **402**, 799–802 (1999).
15. C. A. Choy, C. C. C. Wabnitz, M. Weijerman, P. A. Woodworth-Jefcoats, J. J. Polovina, Finding the way to the top: How the composition of oceanic mid-trophic micronekton groups determines apex predator biomass in the central North Pacific. *Mar. Ecol. Prog. Ser.* **549**, 9–25 (2016).
16. J. M. O'Malley, J. C. Drazen, B. N. Popp, E. Gier, R. J. Toonen, Spatial variability in growth and prey availability of lobsters in the northwestern Hawaiian Islands. *Mar. Ecol. Prog. Ser.* **449**, 211–220 (2012).
17. P. H. Ostrom, A. E. Wiley, H. F. James, S. Rossman, W. A. Walker, E. F. Zipkin, Y. Chikaraishi, Broad-scale trophic shift in the pelagic North Pacific revealed by an oceanic seabird. *Proc. R. Soc. B* **284**, 20162436 (2017).
18. B. N. Popp, B. S. Graham, R. J. Olson, C. C. S. Hannides, M. J. Lott, G. A. López-Ibarra, F. Galván-Magaña, B. Fry, Insight into the trophic ecology of yellowfin tuna, *Thunnus albacares*, from compound-specific nitrogen isotope analysis of proteinaceous amino acids. *Terr. Ecol.* **1**, 173–190 (2007).
19. B. H. Becker, S. R. Beissinger, Centennial decline in the trophic level of an endangered seabird after fisheries decline. *Conserv. Biol.* **20**, 470–479 (2006).
20. B. H. Becker, S. H. Newman, S. Inglis, S. R. Beissinger, Diet–feather stable isotope ($\delta^{15}\text{N}$ and $\delta^{13}\text{C}$) fractionation in Common Murres and other seabirds. *Condor* **109**, 451–456 (2007).
21. Y. Chikaraishi, N. O. Ogawa, Y. Kashiyama, Y. Takano, H. Suga, A. Tomitani, H. Miyashita, H. Kitazato, N. Ohkouchi, Determination of aquatic food-web structure based on compound-specific nitrogen isotopic composition of amino acids. *Limnol. Oceanogr.* **7**, 740–750 (2009).
22. S. E. Lyday, L. T. Ballance, D. B. Field, K. D. Hyrenbach, Shearwaters as ecosystem indicators: Towards fishery-independent metrics of fish abundance in the California Current. *J. Mar. Syst.* **146**, 109–120 (2015).
23. A. E. Wiley, P. H. Ostrom, A. J. Welch, R. C. Fleischer, H. Gandhi, J. R. Southon, T. W. Stafford Jr., J. F. Penniman, D. Hu, F. P. Duvall, H. F. James, Millennial-scale isotope records from a wide-ranging predator show evidence of recent human impact to oceanic food webs. *Proc. Natl. Acad. Sci. U.S.A.* **110**, 8972–8977 (2013).
24. O. A. Sherwood, T. P. Guilderson, F. C. Batista, J. T. Schiff, M. D. McCarthy, Increasing subtropical North Pacific Ocean nitrogen fixation since the Little Ice Age. *Nature* **505**, 78–81 (2014).
25. P. J. Gould, J. F. Piatt, Seabirds of the central North Pacific, in *The Status, Ecology, and Conservation of Marine Birds of the North Pacific*, K. Vermeer, K. T. Briggs, K. H. Morgan, D. Siegel-Causey, Eds. (Canadian Wildlife Service Special Publication, 1993), pp. 27–38.
26. J. Reed, L. Shannon, L. Velez, E. Akoglu, A. Bundy, M. Coll, C. Fu, E. A. Fulton, A. Grüss, G. Halouani, J. J. Heymans, J. E. Houle, E. John, F. Le Loc'h, B. Salihoglu, P. Verley, Y.-J. Shin, Ecosystem indicators—Accounting for variability in species' trophic levels. *ICES J. Mar. Sci.* **74**, 158–169 (2017).
27. K. Wolter, M. S. Timlin, El Niño/Southern Oscillation behaviour since 1871 as diagnosed in an extended multivariate ENSO index (MEI.ext). *Int. J. Climatol.* **31**, 1074–1087 (2011).
28. N. J. Mantua, S. R. Hare, Y. Zhang, J. M. Wallace, R. C. Francis, A Pacific interdecadal climate oscillation with impacts on salmon production. *Bull. Am. Meteorol. Soc.* **78**, 1069–1079 (1997).
29. C. S. Harrison, T. S. Hida, M. P. Seki, Hawaiian seabird feeding ecology. *Wildl. Monogr.* **85**, 3–71 (1983).
30. L. Cardona, I. Álvarez de Quevedo, A. Borrell, A. Aguilar, Massive consumption of gelatinous plankton by Mediterranean apex predators. *PLOS ONE* **7**, e31329 (2012).
31. J. C. McInnes, R. Alderman, M.-A. Lea, B. Raymond, B. E. Deagle, R. A. Phillips, A. Stanworth, D. R. Thompson, P. Catry, H. Weimerskirch, C. G. Suazo, M. Gras, S. N. Jarman, High occurrence of jellyfish predation by black-browed and Campbell albatross identified by DNA metabarcoding. *Mol. Ecol.* **26**, 4831–4845 (2017).
32. K. S. Van Houtan, L. McClenachan, J. N. Kittinger, Seafood menus reflect long-term ocean changes. *Front. Ecol. Environ.* **11**, 289–290 (2013).
33. A. H. Bowers, O. J. Murillo, R. R. Jensen, B. Eslinger, C. Gelzer, On wings of the minimum induced drag: Spanload implications for aircraft and birds. *NASA Tech. Publ.* **2016**, 1–22 (2016).
34. J. J. Polovina, E. Howell, D. R. Kobayashi, M. P. Seki, The transition zone chlorophyll front, a dynamic global feature defining migration and forage habitat for marine resources. *Prog. Oceanogr.* **49**, 469–483 (2001).
35. C. T. Yarnes, J. Herszage, The relative influence of derivatization and normalization procedures on the compound-specific stable isotope analysis of nitrogen in amino acids. *Rapid Commun. Mass Spectrom.* **31**, 693–704 (2017).
36. K. E. Keller, A. D. Anders, S. A. Shaffer, M. A. Kappes, B. Flint, A. Friedlander, Seabirds, in *A Marine Biogeographic Assessment of the Northwestern Hawaiian Islands*. NOAA Technical Memorandum NOS NCCOS 84, A. Friedlander, K. Keller, L. Wedding, A. Clarke, M. Monaco, Eds. (National Oceanic and Atmospheric Administration, 2009), pp. 235–274.
37. M. de L. Brooke, The food consumption of the world's seabirds. *Proc. R. Soc. Lond. B Biol. Sci.* **271**, S246–S248 (2004).
38. D. K. Danckwerts, C. D. McQuaid, A. Jaeger, G. K. McGregor, R. Dwight, M. Le Corre, S. Jaquemet, Biomass consumption by breeding seabirds in the western Indian Ocean: Indirect interactions with fisheries and implications for management. *ICES J. Mar. Sci.* **71**, 2589–2598 (2014).
39. D. E. Galván, C. J. Sweeting, W. D. K. Reid, Power of stable isotope techniques to detect size-based feeding in marine fishes. *Mar. Ecol. Prog. Ser.* **407**, 271–278 (2010).
40. Z. A. Doubleday, T. A. A. Prowse, A. Arkhipkin, G. J. Pierce, J. Semmens, M. Steer, S. C. Leporati, S. Lourenço, A. Quetglas, W. Sauer, B. M. Gillanders, Global proliferation of cephalopods. *Curr. Biol.* **26**, R406–R407 (2016).
41. P. G. K. Rodhouse, G. J. Pierce, O. C. Nichols, W. H. H. Sauer, A. I. Arkhipkin, V. V. Laptikhovskiy, M. R. Lipiński, J. E. Ramos, M. Gras, H. Kidokoro, K. Sadayasu, J. Pereira, E. Lefkaditou, C. Pita, M. Gasalla, M. Haimovici, M. Sakai, N. Downey, Environmental effects on cephalopod population dynamics: Implications for management of fisheries. *Adv. Mar. Biol.* **67**, 99–233 (2014).
42. D. C. Schneider, J. F. Piatt, Scale-dependent correlation of seabirds with schooling fish in a coastal ecosystem. *Mar. Ecol. Prog. Ser.* **32**, 237–246 (1986).
43. W. A. Montevecchi, V. L. Birt, D. Cairns, Dietary changes of seabirds associated with local fisheries failures. *Biol. Oceanogr.* **5**, 153–161 (1988).
44. E. T. Kai, S. Benhamou, C. D. van der Lingen, J. C. Coetzee, L. Pichegru, P. G. Ryan, D. Grémillet, Are Cape gannets dependent upon fishery waste? A multi-scale analysis using seabird GPS-tracking, hydro-acoustic surveys of pelagic fish and vessel monitoring systems. *J. Appl. Ecol.* **50**, 659–670 (2013).
45. K. J. Benoit-Bird, B. C. Battaile, S. A. Heppell, B. Hoover, D. Irons, N. Jones, K. J. Kuletz, C. A. Nordstrom, R. Paredes, R. M. Suryan, C. M. Waluk, A. W. Trites, Prey patch patterns predict habitat use by top marine predators with diverse foraging strategies. *PLOS ONE* **8**, e53348 (2013).
46. H. Weimerskirch, D. P. Filippi, J. Collet, S. M. Waugh, S. C. Patrick, Use of radar detectors to track attendance of albatrosses at fishing vessels. *Conserv. Biol.* **32**, 240–245 (2017).
47. F. Hertel, L. T. Ballance, Wing ecomorphology of seabirds from Johnston Atoll. *Condor* **101**, 549–556 (1999).
48. J. R. Krebs, N. B. Davies, J. Parr, *An Introduction to Behavioural Ecology* (Blackwell Scientific Publications, 1993).
49. W. S. Cleveland, S. J. Devlin, Locally weighted regression: An approach to regression analysis by local fitting. *J. Am. Stat. Assoc.* **83**, 596–610 (1988).
50. R. Froese, D. Pauly, *FishBase* (2017); www.fishbase.org.
51. B. Stock, B. Semmens, E. Ward, A. Parnell, A. Jackson, D. Phillips, J. Moore, S. Bearhop, R. Inger, MixSIAR: Bayesian Mixing Models in R. *MixSIAR User Manual* (2013).
52. B. C. Stock, B. X. Semmens, Unifying error structures in commonly used biotracer mixing models. *Ecology* **97**, 2562–2569 (2016).
53. E. Di Lorenzo, N. Schneider, K. M. Cobb, P. J. S. Franks, K. Chhak, A. J. Miller, J. C. McWilliams, S. J. Bograd, H. Arango, E. Curchitser, T. M. Powell, P. Rivière, North Pacific

- Gyre Oscillation links ocean climate and ecosystem change. *Geophys. Res. Lett.* **35**, L08607 (2008).
54. B. Huang, V. F. Banzon, E. Freeman, J. Lawrimore, W. Liu, T. C. Peterson, T. M. Smith, P. W. Thorne, S. D. Woodruff, H.-M. Zhang, Extended reconstructed sea surface temperature version 4 (ERSST.v4). Part I: Upgrades and intercomparisons. *J. Climate* **28**, 911–930 (2015).
55. A. Liaw, M. Wiener, Classification and regression by randomForest. *R News* **2**, 18–22 (2002).
56. T. Hastie, R. Tibshirani, J. Friedman, *The Elements of Statistical Learning* (Springer, 2009), pp. 9–41.
57. L. Breiman, Random forests. *Mach. Learn.* **45**, 5–32 (2001).
58. D. Pauly, The *Sea Around Us* Project: Documenting and communicating global fisheries impacts on marine ecosystems. *AMBIO* **36**, 290–295 (2007).

Acknowledgments: We thank C. Yarnes for performing the CSIA-AA analyses; V. Lam for providing fishery data from the SAU database; A. Copenhaver, E. Frederickson, and E. Schick for providing logistical support; C. White for advising on the R code and modeling approach; and S. Jorgensen, A. Boustany, J. Moxley, A. Choy, A. Copenhaver, A. Johnson, and three anonymous reviewers for improving earlier versions of this manuscript. This research was

performed under USFWS permit nos. MB052060-0 and MB180283-1 to K.S.V.H. and K.D.H. All research followed the Institutional Animal Care and Use Committee criteria under NOAA and Hawaii Pacific University. **Funding:** This work was supported, in part, by a Presidential Early Career Award for Scientists and Engineers to K.S.V.H. **Author contributions:** M.E.H., K.D.H., and K.S.V.H. designed the study and collected seabird data. T.O.G. and K.S.V.H. analyzed data, prepared figures, and wrote the manuscript. T.O.G. designed the models and wrote the R code. All authors reviewed the manuscript. **Competing interests:** The authors declare that they have no competing interests. **Data and materials availability:** All data needed to evaluate the conclusions in the paper are present in the paper and/or the Supplementary Materials. Additional data related to this paper may be requested from the authors.

Submitted 14 July 2017

Accepted 12 January 2018

Published 14 February 2018

10.1126/sciadv.aao3946

Citation: T. O. Gagne, K. D. Hyrenbach, M. E. Hagemann, K. S. Van Houtan, Trophic signatures of seabirds suggest shifts in oceanic ecosystems. *Sci. Adv.* **4**, eaao3946 (2018).